

Time-dependent Hartree-Fock calculation of the escape width of the giant monopole resonance in ^{16}O

J. M. Pacheco*

The Niels Bohr Institute, University of Copenhagen, Copenhagen, Denmark

E. Maglione

Dipartimento di Fisica "Galileo Galilei," Padova

and Istituto Nazionale di Fisica Nucleare Laboratori Nazionali di Legnaro, Legnaro, Italy

R. A. Broglia

The Niels Bohr Institute, University of Copenhagen, Copenhagen, Denmark

and Dipartimento di Fisica, Università di Milano and Istituto Nazionale di Fisica Nucleare Sezione di Milano, Milano, Italy

(Received 7 December 1987)

The damping of the giant monopole resonance in ^{16}O is calculated within the framework of the time-dependent Hartree-Fock approximation. The strength function contains two peaks, centered at around 25 and 33 MeV, with escape widths of ~ 11 and ~ 2 MeV, associated with the $1p(0p)^{-1}$ and $1s(0s)^{-1}$ configurations, respectively.

A giant vibration can be viewed as a state of a correlated particle above the Fermi surface and a hole in the Fermi sea, carrying a large fraction of the energy-weighted sum rule (EWSR).

There are three basic mechanisms which can weaken or even obliterate the correlation: (i) The strength of the vibration can be spread over many particle-hole components; (ii) giant resonances (GR), being located above particle threshold, can decay by proton and neutron emission; and (iii) giant vibrations are imbedded in a spectrum of high-level density to which they couple, decaying eventually into the compound nucleus.

The spreading within the space of particle-hole configurations is known, in the case of infinite media, as Landau damping.¹ In heavy, finite nuclei it gives rise to a breaking of the strength of the vibration rather than to an actual damping.² In the case of light nuclei, where the unperturbed particle-hole excitations can be in the continuum, the phenomenon is very similar to that observed in infinite systems. In any case, for economy we will still characterize it by a single quantity Γ_L .

Particle decay spreads the strength of the different peaks of the giant resonance, and is measured by the escape width Γ^\uparrow , while coupling of the giant resonances to the compound nucleus is controlled by the damping width Γ^\downarrow , the total width Γ_t being the sum of the three contributions Γ^\uparrow , Γ_L , and Γ^\downarrow .

The two first damping mechanisms, labeled (i) and (ii), are present already at the level of the random-phase approximation (RPA), while a description of the damping width Γ^\downarrow requires going beyond mean-field theory.³ It can then seem surprising that while little is known about both Γ^\uparrow and Γ_L , a satisfactory understanding of Γ^\downarrow exists. This is because the treatment of the continuum is always cumbersome,⁴ and because the density distribution of the unperturbed particle-hole energies is strongly dependent on scarcely known details of the residual force,

in particular those components responsible for the existence of the spin-orbit potential. On the other hand, Γ^\downarrow is controlled by selected doorway states. Consequently, once the correct degrees of freedom have been identified, the resulting damping width is essentially independent of the residual force.⁵

Because of the marked shell structure and the relatively few single-particle bound states found in light nuclei, Γ_t is expected to be controlled by Γ^\uparrow and Γ_L , while their role seems to be, as a rule, not important in heavy nuclei.

Time-dependent Hartree-Fock approximation (TDHF) has been shown⁶ to be a useful tool to describe particle emission from giant resonances. In the present paper, and starting from the results obtained in Ref. 6, we use the same method to investigate in detail the mechanism of particle emission, therefore discriminating the roles played by Γ^\uparrow and Γ_L in the attenuation of the amplitude of the giant monopole resonance (GMR) in ^{16}O .

The new points presented in this paper as compared to Ref. 6 are (i) the separation of the density oscillations in the contributions arising from the different orbitals; (ii) the study of the time dependence of the amplitude of the different components in the collective wave function; and (iii) the extraction of the escaping widths Γ^\uparrow from these quantities, as well as from the time dependence of the mean-square radii associated with the different densities. These results will allow us to conclude that essentially all the width of the strength function obtained in Ref. 6 is due to particle emission, Landau damping playing a small role in the damping process (cf. also Ref. 7).

The effective force used in the calculations reads⁶

$$V(\mathbf{r}_1, \mathbf{r}_2) = \left[t_0 + \frac{1}{6} t_3 \rho \left(\frac{\mathbf{r}_1 + \mathbf{r}_2}{2} \right) \right] \delta(\mathbf{r}_1 - \mathbf{r}_2), \quad (1)$$

with the values $t_0 = -1000$ (MeV fm³) and $t_3 = 15000$ (MeV fm⁶) for the Skyrme parameters, leading to a nu-

clear matter compressibility of 430 MeV. The Hartree-Fock (HF) ground state of ^{16}O is found to have a binding energy of -155 MeV, a root-mean-square radius of 2.43 fm, and the bound single-particle spectrum quoted in Table I. The TDHF equations were solved in coordinate space within a box of 40 fm.

An isoscalar monopole vibration was induced in the system by boosting the static HF single-particle wave functions with the operator

$$\exp(-iKr^2),$$

where

$$K = 0.032 \text{ fm}^{-2},$$

corresponding to an excitation energy of 8 MeV. A boost with an excitation energy ten times smaller gives essentially the same results as those presented below, indicating that the system is in the linear-response regime.

The main properties of the unperturbed monopole response are schematically shown in Fig. 1. The only bound 1p-1h excitation, $1s(0s)^{-1}$, lies at an excitation energy of 31.7 MeV, while there is a continuum of states starting at ~ 19 MeV for 1p-1h configurations with a hole in the $0p$ state.

Solving the TDHF equations, the wave function $\Phi(r, t)$ is obtained. At $t = 0$, $\Phi(r, 0)$ can be expanded in terms of the different static HF configurations. For the situation under consideration, the probabilities associated with the ground state, the 1p-1h and the 2p-2h configurations, are 0.78, 0.20, and 0.02, respectively. They are rather constant as a function of time [cf. Fig. 2(a)]. This reflects the very weak coupling existing between 1p-1h and 2p-2h configurations, which seems to imply a small value for Γ^\downarrow . In fact, these couplings (cf. Sec. 8 of Ref. 8) constitute the doorway mechanism for producing the damping width of the GR.⁵

Because of the very large energy difference existing between the static HF $0s$ and $0p$ bound states, we find the density oscillations in time to display two main frequencies associated with excitations based on these two different single-particle states. Therefore, we will consider them separately. In particular, we shall make use of the partial L densities, $s(L=0)$ and $p(L=1)$, defined as

$$\rho_L(r, t) = 4(2L+1) |\varphi_L(r, t)|^2, \quad (2)$$

where $\varphi_L(r, t)$ ($L=0, 1$) are the time-dependent single-particle wave functions evolved from the corresponding static HF single-particle wave functions $\psi_L(r)$.

The contributions to the mean-square radius coming from the particles in the s and p wave functions are shown in Fig. 3(b). A marked increase of the radius is ob-

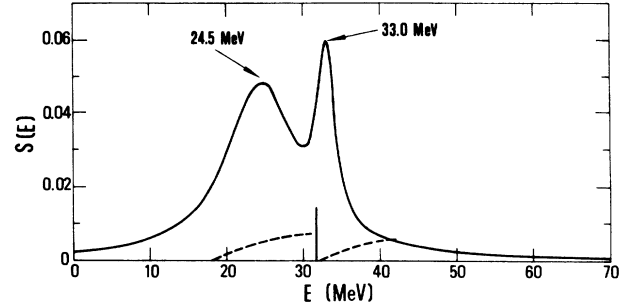


FIG. 1. Schematic representation of the strength function for the monopole boost. The vertical line represents the static HF $1s(0s)^{-1}$ particle-hole excitation; the two dashed lines illustrate the continuum for static HF 1p-1h excitations, with a hole in the $0s$ and $0p$ states. The solid curves correspond to Breit-Wigner curves centered at the obtained values for the energies of the two modes (24.5 and 33.0 MeV), and with the calculated widths $\Gamma(p) = 12$ MeV and $\Gamma(s) = 2.5$ MeV.

served, which can be attributed to the emission of particles.⁶ Extracting from these results the monotonic increase, one can calculate the centroid and the summed $\Gamma = \Gamma^\uparrow + \Gamma_L$ average attenuation width of the oscillations [cf. Fig. 3(c)]. They are schematically shown in Fig. 1, and are equal to $\Gamma(p) \simeq 12$ MeV and $\Gamma(s) \simeq 2.5$ MeV. The large difference between these two numbers is related to the fact that $\hbar\omega_p$ lies 6 MeV above the starting of the continuum, while $\hbar\omega_s$ is just at threshold, as we shall discuss in the following.

Figures 3(a) and 2(b) display the time dependence of the particle emission process. From Fig. 3(a) one can observe that particles are shaken off from the nucleus with largest probability at the time of maximum expansion, the probability being smallest at the other extreme of the oscillation, when the nucleus has reached its minimum radius. The process of particle escape can be seen to extend over few oscillations, the more energetic particles being emitted first, lending support to an energy dependence of the decaying width. The average velocity of the emitted particles was estimated by considering the time displacement of the main peaks in Fig. 3(a), leading to the values $v_s/c \simeq 0.15$ and $v_p/c \simeq 0.22$, where c is the velocity of light (cf. also Ref. 6).

Figure 2(b) gives further insight into the mechanism of particle decay taking place from the peak associated with the excitation of s particles. Because the unperturbed $1s$ state is bound, all particle decay will go through the $ns(0s)^{-1}$ configurations with $n > 1$. The vibrational mode then gets depopulated from its main component (solid line) as a function of time, as the unbound components go on losing particles. This is because the coherence between the particle and the hole will maintain constant the relative values of the different amplitudes participating in the vibration. Consequently, the $1s(0s)^{-1}$ component decreases as the normalization of the mode decreases. An exponential fit to the full drawn curve displayed in Fig. 2(b) gives the value $\Gamma(s) \simeq 2.5$ MeV for the damping of the state, in agreement with the value obtained above.

TABLE I. Static Hartree-Fock single-particle spectrum. In the case of the p state, the starting energy for the continuum of states within the box is given.

Static HF single-particle spectrum					
Single-particle level	$0s$	$0p$	$0d$	$1s$	$1p$
Energy (MeV)	-32.2	-18.2	-2.4	-0.5	1.4

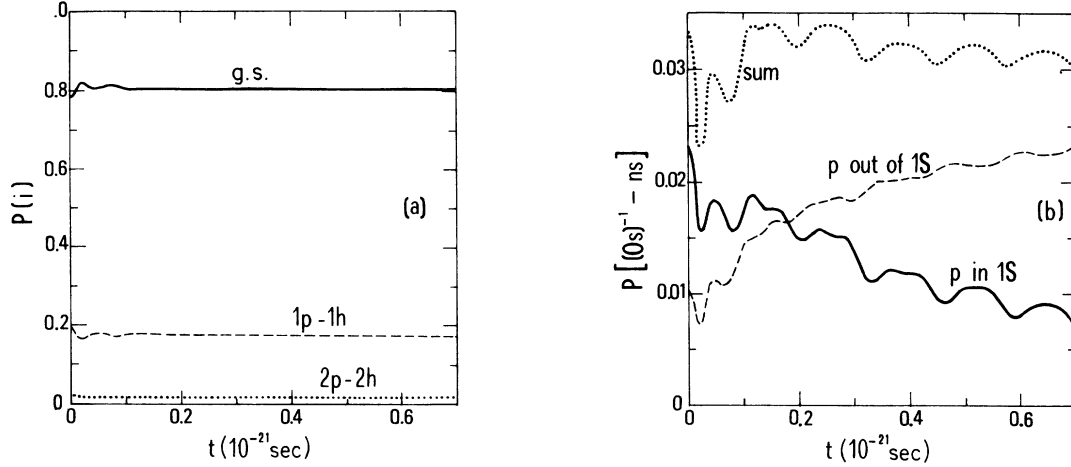


FIG. 2. Probabilities for different configurations as a function of time: (a) The upper curve shows the probability for the system to be in the HF ground state as a function of time. The middle curve displays the corresponding probability to have any static HF 1p-1h excitation in time. The lower curve gives the probability of having 2p-2h configurations. (b) The probability of having any 1p-1h excitation, with a hole in the static HF 0s state (upper curve) is decomposed into two parts: the one in which the particle in the 1s state (solid curve) and the part where the particle is in the continuum (lower dashed curve). An exponential fit to the solid curve leads to the value $\Gamma(s) \approx 2.5$ MeV for the decaying rate of the probability.

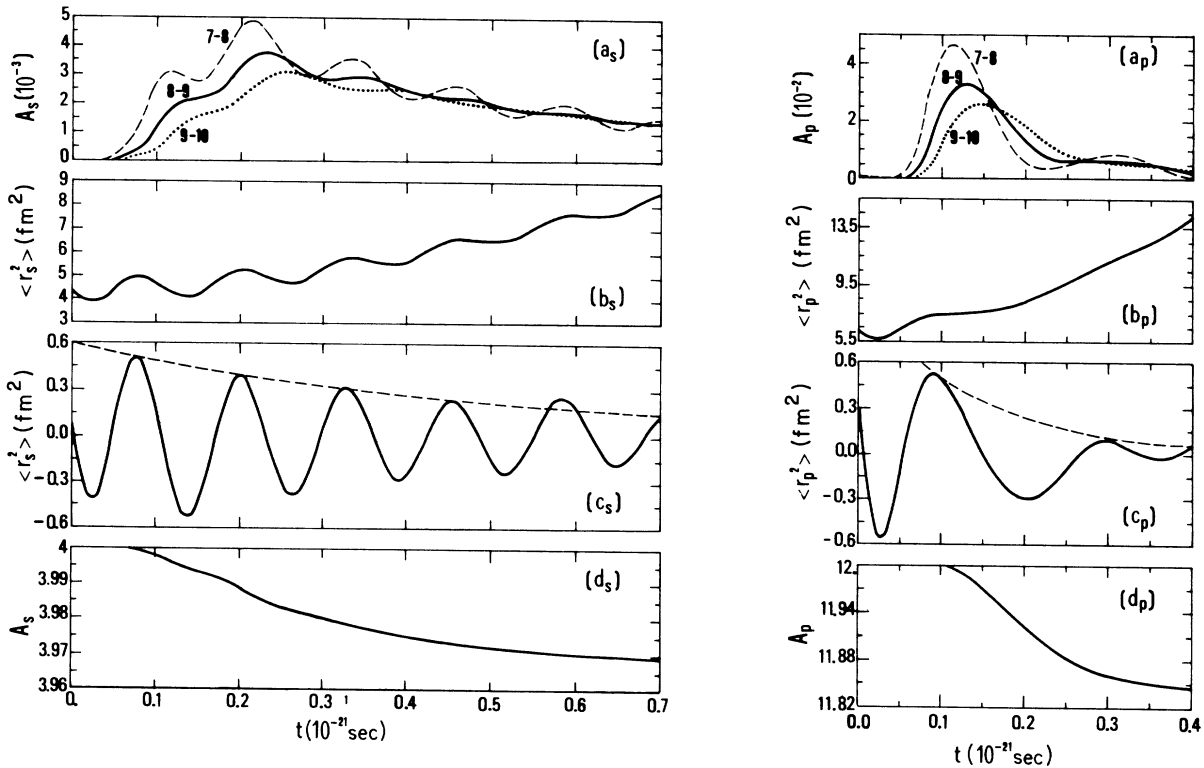


FIG. 3. Time evolution of the mean-square radius and the number of particles. On the left is shown the time evolution of the number of particles and of the mean-square radius, corresponding to the s ($L=0$) mode. On the right the time evolution of the same quantities is plotted for the p ($L=1$) mode [see Eq. (2)]. (a) Number of particles enclosed in spherical layers of different radii. The s and p densities, defined in Eq. (2), were integrated in three different regions, delimited by the three pairs of spherical surfaces with radii (7,8), (8,9), and (9,10) fm, respectively. The different curves display both the motion and the spreading of the wave packets associated with the emitted particles. (b) Total mean-square radii as a function of time. Because the integration volume extends to the whole box (40 fm), these mean-square radii receive contributions from the emitted particles. Subtracting the associated monotonic increase isolates the oscillatory behavior. (c) The oscillatory behavior of the subtracted mean-square radii is clearly damped, as illustrated by the dashed lines, obtained by fitting the corresponding extrema with the function $Ae^{-\Gamma t/2\hbar}$. The values obtained are $\Gamma(s) \approx 2.5$ MeV and $\Gamma(p) \approx 12$ MeV. (d) The number of particles inside a sphere of radius R_0 ($R_0=8$ and 12 fm in the case of the s and p densities, respectively), centered at the nuclear origin, is displayed as a function of time. A fit to these curves with the function (3) leads to the values $\Gamma(s) \approx 2.2$ MeV and $\Gamma(p) \approx 11.0$ MeV.

In what follows we will attempt to disentangle the roles played by Γ^\dagger and Γ_L in the average attenuation widths calculated above. This is done by studying the change of the number of particles enclosed within a sphere containing the nucleus as a function of time [cf. Fig. 3(d)]. From these results, one can extract an average escape width through the relation (cf. also Ref. 7)

$$n_i(t) = \Delta n_i e^{-\Gamma_i^\dagger t/\hbar} + n_i(\infty) \quad (i = s, p). \quad (3)$$

The resulting values for Γ^\dagger are $\Gamma_s^\dagger \simeq 2.2$ MeV and $\Gamma_p^\dagger \simeq 11.0$ MeV, respectively. When compared with the previous values, obtained by fitting the curves of Figs. 2(b) and 3(c), they show that Γ_L is small, as one would expect from more general arguments.²

From the results shown in Fig. 2 one can evaluate the number of particles which were promoted to excited static HF configurations by boosting the system. This result coincides with that extracted estimating $n(\infty)$ from Fig. 3(d), by fitting the tails of these curves. This result again

indicates that the central process contributing to the attenuation of the modes is particle emission.

A schematic TDHF calculation of the GMR of ^{16}O gives two peaks which are mainly associated with the excitation of s and p particles. The width associated with those states is of the order of $\Gamma_p \simeq 12.0$ MeV and $\Gamma_s \simeq 2.5$ MeV. By investigating the relation between the number of particles which leave the nucleus as a function of time and the attenuation of the monopole oscillations of the system, one finds that most of the reported widths are due to particle emission, with the resulting values of $\Gamma_s^\dagger \simeq 2.2$ MeV and $\Gamma_p^\dagger \simeq 11.0$ MeV, both Γ^\dagger and Γ_L being small.

We are indebted to B. S. Nilsson for providing us the HF codes. Discussions with B. Mottelson and P. F. Bortignon are gratefully acknowledged. One of us (J.M.P.) would like to thank Y. R. Shimizu for many comments and suggestions, as well as the Fundação Calouste Gulbenkian for financial support.

*On leave of absence from the University of Coimbra, Portugal.

¹D. Pines and P. Nozières, *Theory of Quantum Liquids* (Benjamin, New York, 1966).

²C. Fiolhais, Ann. Phys. (N.Y.) **171**, 186 (1986); J. J. Griffin and M. Dworzecka, Phys. Lett. **156B**, 139 (1985); C. Yannouleas, Nucl. Phys. **A439**, 336 (1985).

³J. Negele, Rev. Mod. Phys. **54**, 913 (1982).

⁴S. Shlomo and G. F. Bertsch, Nucl. Phys. **A243**, 507 (1975); K. F. Liu and N. Van Giai, Phys. Lett. **65B**, 23 (1976); N. Van Giai and H. Sagawa, Nucl. Phys. **A371**, 1 (1981).

⁵G. F. Bertsch, P. F. Bortignon, and R. A. Broglia, Rev. Mod. Phys. **55**, 287 (1983).

⁶S. Stringari and D. Vautherin, Phys. Lett. **88B**, 1 (1979).

⁷Ph. Chomaz, N. Van Giai, and S. Stringari, Phys. Lett. **B 189**, 375 (1987).

⁸A. Kerman, in *Elementary Modes of Excitation in Nuclei*, Proceedings of the International School of Physics "Enrico Fermi," Course LXIX, Varenna, 1976, edited by A. Bohr and R. A. Broglia (North-Holland, Amsterdam, 1977), p. 135.